ATLAS NOTE

ATLAS-CONF-2011-030

March 22, 2011

In-situ jet energy scale and jet shape corrections for multiple interactions in the first ATLAS data at the LHC

The ATLAS collaboration

Abstract

In-situ methods are presented for subtracting contributions to the measured jet energy due to additional proton-proton interactions (pile-up). The performance of these methods is evaluated using the first data collected with the ATLAS detector in proton-proton collisions at the LHC, at a center-of-mass energy of $\sqrt{s} = 7$ TeV. These additional collisions deposit diffuse, soft radiation in the calorimeter that is uncorrelated with jets from the primary interaction of interest. This introduces an energy offset which can, on average, be subtracted from the measured jet energy, and two methods for deriving and applying energy offset corrections are discussed. These corrections reduce the uncertainty in the jet energy scale due to pile-up to approximately 100 MeV per additional interaction vertex, an improvement by nearly a factor of five over the measured bias prior to the correction. A significant influence of pile-up on the differential jet shape of up to 40% near the nominal radius of the jet is also demonstrated and corrections based on the derived energy offset are presented.

1 Introduction

The high luminosity for which the LHC was designed comes at the cost of multiple extraneous (to the collision of interest) proton-proton (pp) interactions occurring at each bunch crossing [1, 2]. These interactions – collectively called "pile-up" – induce an uncorrelated background of soft, diffuse energy in the calorimeter that offsets measurements of jets from the primary interaction of interest. In the ATLAS detector [3], this offset is approximately 0.5 GeV per additional vertex in the central region prior to hadronic calibration and can impact jet shape and structure measurements significantly. Far from being only a long-term future consideration, pile-up has already become an important issue at the LHC.

This note presents *in-situ* methods to correct jets for effects due to pile-up interactions. The *relative* effect of additional pp interactions on the jet energy is measured with respect to events[1] with only a single hard-scattering using two approaches: a purely calorimeter-based technique, where the uncorrected energy density in calorimeter towers is measured for each additional observed interaction independent of the jet finding, and a so-called "track-jet" technique. The latter method selects calorimeter jets via matched track-jets constructed directly from charged particle tracks originating from only the identified hard-scattering. Such track-jets can be effectively separated from pile-up interactions via the longitudinal position along the beam line. Track-jets are thus unaffected by pile-up and provide a reference against which to compare calorimeter-jets, which are affected. Both techniques utilize relative measurements in order to estimate the offset due to pile-up and therefore, by construction, do not correct for the underlying event or for any impact on the jet energy resolution.

Several other strategies for mitigating the effects of pile-up on jets have been studied using, for example, the jet area [4] and the complementary cone approaches [5]. This note focuses on the tower-based and track-jet methods, which offer well-understood systematic uncertainties in the very early data. Additionally, the relative nature of the correction is an important difference compared to the jet area-based method, as it allows for a factorized procedure for pile-up and underlying event corrections, which are based on fundamentally different physics processes. Nonetheless, the strategy of using the number of observed interactions to scale the correction event-by-event in the tower-based method is analogous to the average event-by-event background energy density measurement in the jet area-based approach.

The note is organized as follows. Section 2 describes the overall strategy adopted to correct for the uncorrelated, diffuse energy added to jets as a result of pile-up. In Section 3, the data used for these studies, and for event and object selections, are discussed. The two methods by which the effect of additional interactions on jets is measured are reported separately in Sections 4 and 5, where the derived corrections are also presented for each method. The results of applying the tower-based offset correction to the data, and its effect on jet shapes, are then shown in Section 6. In Section 7, the utility of the current approaches is reviewed and future possibilities for pile-up corrections are discussed.

2 Strategy to correct for pile-up contributions

The application of the transverse energy (E_{T}) offset correction can be written generically as

$$E_T^{\text{corrected}} = E_T^{\text{uncorrected}} - \mathscr{O}(\eta, N_{\mathrm{PV}}, \tau_{\text{bunch}}), \tag{1}$$

[1] The phrase event refers to the triggered pp bunch crossing, which may include multiple such collisions occurring simultaneously as well as effects from previous pp collisions.

where $\mathscr{O}(\eta, N_{\mathrm{PV}}, \tau_{\mathrm{bunch}})$ is derived as a function of pseudorapidity[2], η, due to the underlying differential particle spectrum and the variation in the calorimeter geometry. The number of reconstructed primary vertices, N_{PV}, serves as the event-by-event metric by which to estimate the amount of pile-up, and thus the response of the calorimeter to multiple interactions. Lastly, τ_{bunch} is the spacing between consecutive colliding proton bunches, which may affect the response of the calorimeter at high luminosity. The dependence on τ_{bunch} is explicitly allowed for due to the possibility of pile-up contributions from previous pp bunch crossings for closely spaced bunches. Although this study does not investigate the impact of various τ_{bunch} on the offset, it will be an important consideration for the 2011-2012 LHC run as the number of bunches is increased and the spacing between consecutive bunches is reduced. The correction is assumed to be independent of the jet energy, as contributions due to pile-up are uncorrelated with the proton-proton collision which produces the jet of interest. This assumption will be tested using the track-jet approach (see Section 5). In the tower-based and track-jet approaches, a reference class of events is defined by a given number of interactions, $N_{\mathrm{PV}}^{\mathrm{ref}}$, such that

$$\mathscr{O}(\eta, N_{\mathrm{PV}}) = \langle E_T^{\mathrm{measured}}(\eta, N_{\mathrm{PV}})\rangle - \langle E_T^{\mathrm{reference}}(\eta, N_{\mathrm{PV}}^{\mathrm{ref}})\rangle. \quad (2)$$

For the 2010 data, events with only a single reconstructed primary interaction are used as the reference, such that $N_{\mathrm{PV}}^{\mathrm{ref}} = 1$.

3 Data sample and event selection

The influence of several distinct periods of machine configuration and detector operation are present in the first 40 pb^{-1} of data collected by ATLAS. As the LHC commissioning progressed, changes in the beam optics and proton bunch parameters resulted in clear changes in the number of pile-up interactions per bunch crossing. Figure 1 shows the evolution of the peak number of interactions derived from the online luminosity measurement and assuming an inelastic pp cross section of 71.5 mb [6]. The very first data were essentially devoid of multiple pp interactions until the optics of the accelerator beam (specifically β^*) were changed in order to decrease the transverse size of the beam and increase the luminosity[3] [7]. This change alone raised the fraction of events with at least two observed interactions from less than 2% to between 8-10% (May-June). A further increase occurred when the number of protons in each proton bunch (ppb, or the bunch intensity) was increased from approximately $5-9\times10^{10}$ to 1.15×10^{11} ppb. Since the number of pp collisions per bunch crossing is proportional to the square of the bunch intensity, the fraction of events with pile-up increased to more than 50% for runs between June and September. Finally, continued beam intensity enhancement slowly raised the average number of interactions per crossing to more than three by the end of the pp run in November.

3.1 Event selections

Data used for this study were collected during the period from June to August 2010. In total, an integrated luminosity of 0.34 pb$^{-1}\pm0.038$ pb^{-1} is used to derive the corrections and to assess the performance in the data. An average primary vertex multiplicity of $\langle N_{\mathrm{PV}}\rangle = 1.5$ is observed for this period.

Events are selected using the first level (L1) calorimeter triggers, consisting of both electromagnetic energy and jet triggers. Raw tower energy distributions used in the measurement of the correction (see

[2]The ATLAS reference system is a Cartesian right-handed coordinate system, with nominal collision point at the origin. The anti-clockwise beam direction defines the positive z-axis, with the x-axis pointing to the center of the LHC ring. The pseudorapidity is defined as $\eta = -\ln(\tan(\theta/2))$, where the polar angle θ is taken with respect to the positive z direction. The rapidity is defined as $y = 0.5\times\ln[(E+p_z)/(E-p_z)]$, where E denotes the energy and p_z is the component of the momentum along the beam direction. The azimuthal angle ϕ is defined in the usual way.

[3]The parameter β^* is the value of the β-function at the collision point and smaller values of β^* implies a smaller physical size of the beams and thus a higher instantaneous luminosity.

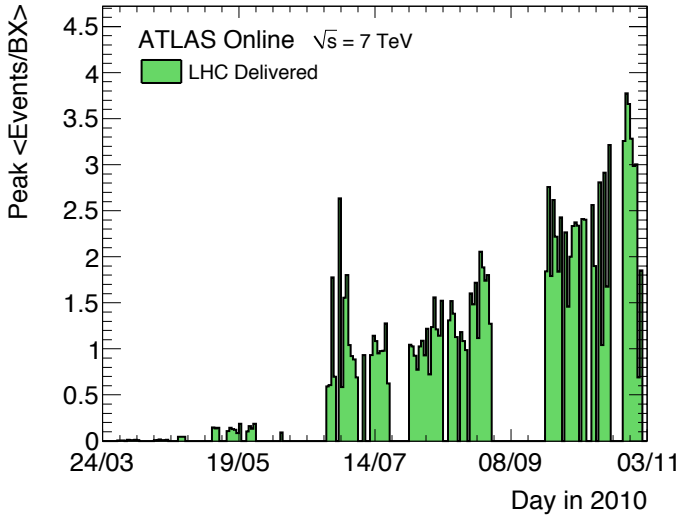

Figure 1: The peak number of interactions per bunch crossing ("BX") as measured online by the ATLAS luminosity detectors [6]. In order to calculate the equivalent mean number of interactions, an inelastic cross-section of $\sigma_{\text{inel}} = 71.5$ mb is assumed.

Section 4) are obtained from the inclusive set of events selected with these triggers. The validation of the correction and the derivation of the track-jet offset correction (discussed in Section 5) require that events pass a single jet trigger (so-called "L1_J15"), which has its 100% efficiency plateau at a reconstructed jet transverse energy of approximately $E_{\text{T}}^{\text{jet}} \geq 70$ GeV [8]. For these studies, the leading jet is not used, so as not to incur any bias due to using the jet that triggered the event.

3.2 Object definitions and selections

For all results, the anti-k_t jet algorithm [9] is used as implemented in the `fastjet` package [10] with a distance parameter of $R = 0.6$. Both calorimeter towers and topological clusters at the electromagnetic (EM) scale are used as inputs in the jet finding and reconstruction. Towers are static, $\Delta\eta \times \Delta\phi = 0.1 \times 0.1$ grid elements, whereas topological clusters (or "topoclusters") are three dimensional, dynamic collections of calorimeter cells with noise suppression applied [11]. The same noise suppression is also applied to the calorimeter towers which are used to reconstruct tower jets. No noise suppression is applied when deriving the offset correction in order to remain sensitive to low energy depositions that may not rise above threshold except inside of a jet (so-called "zero-suppression"). Studies of the effect of pile-up on the calibrated $E_{\text{T}}^{\text{jet}}$, shown in Section 5, utilize the p_T^{jet}- and η^{jet}-dependent Monte Carlo (MC)-based jet energy scale calibration, referred to as the EM+JES [12] scale.

Jets built from charged particle tracks originating from the pp collision of interest – so-called "track-jets" – are used to define a calorimeter jet selection that is insensitive to the effects of pile-up and are discussed in Sections 5 and 6. The Inner Detector (ID) is used to reconstruct these tracks [3] and covers the range up to $|\eta| < 2.5$. The track reconstruction efficiency ranges from 78% at $p_T^{\text{track}} = 500$ MeV to more than 85% above 10 GeV, averaged across the full η coverage [13]. Track-jets are formed using tracks with $p_T^{\text{track}} > 500$ MeV as input to the standard anti-k_t jet algorithm, also with a distance parameter of $R = 0.6$. However, since the tracking efficiency falls significantly above $|\eta| > 2.2$, the calorimeter jet selection requires $|\eta^{\text{jet}}| < 1.9$ prior to matching to track-jets. The resulting track-jets must have at least two constituent tracks and a total $p_T^{\text{track-jet}} > 3$ GeV.

Finally, for all studies, the primary vertex multiplicity (N_{PV}) is measured by counting vertices in the event that are consistent with the measured interaction region [14,15], while excluding secondary vertices that have a significant distance from the beam line. The collision of interest is identified as the primary vertex with the maximum $\Sigma(p_T^{\mathrm{track}})^2$ where the sum runs over all tracks used in the vertex fit. Each vertex is required to contain at least five tracks with $p_T^{\mathrm{track}} > 150$ MeV. This renders the contribution from fake vertices due to beam backgrounds negligible.

4 Tower-based offset correction

The primary approach to correcting for pile-up in jets is based upon the average energy deposited in the calorimeter towers for each additional primary vertex, N_{PV}, as a function of η. This so-called tower-based method provides an energy density grid derived from all towers in the event to evaluate the offset. The jet energy correction for each jet is proportional to the number of constituent towers in the jet, as this provides a clear geometric definition for the application of the correction. For jets built directly from dynamically-sized topological clusters, for which no clear geometric definition is available, a model is used that describes the average area of a jet in terms of the equivalent number of constituent towers. In this way, the correction can be extended to jet algorithms whose inputs are not calorimeter towers. This is discussed in Section 4.2.

4.1 Constituent tower multiplicity of jets

The average multiplicity of noise-suppressed towers in jets provides information on both the jet composition and the extent to which that composition may be augmented by the presence of pile-up. Previous studies [16] have shown that slight discrepancies exist between the data and Monte Carlo, even in this very simple measure of jet composition. It is therefore crucial that any correction that relies on such properties is derived *in-situ*. In the case of the offset correction, the mean constituent tower multiplicity can be used for an extrapolation of the tower-based offset correction to various jet resonstruction methods, e.g. topological cluster jets.

Figure 2 depicts the average noise-suppressed constituent tower multiplicity for an inclusive jet selection with $p_T > 7$ GeV. The shape of the constituent tower multiplicity distribution is governed by the change in physical size of towers for a constant size in pseudorapidity, as well as by differences in the noise spectrum for the various calorimeters and sampling regions. The constituent tower multiplicity distribution is used to translate the tower-level offset into a jet-level offset, while the known p_T and N_{PV} dependencies are neglected. The resulting systematic uncertainty will be discussed in Section 5.

4.2 Tower-based offset at tower-level and jet-level

The foundation of the offset correction is the measurement of the additional transverse energy contributed to a given tower for each additional observed interaction in the event. The EM scale tower-based offset is derived by measuring the average tower transverse energy without hadronic energy calibration for all towers in events with $N_{\mathrm{PV}} = 1,2,...N$ and comparing directly to events with $N_{\mathrm{PV}}^{\mathrm{ref}} = 1$. The resulting "tower-level offset" is shown in Figure 3(a) for $1 \leq N_{\mathrm{PV}} \leq 5$ and is defined as

$$\mathscr{O}_{\mathrm{tower-based}}(\eta, N_{\mathrm{PV}}) = \langle E_T^{\mathrm{tower}}(\eta, N_{\mathrm{PV}}) \rangle - \langle E_T^{\mathrm{tower}}(\eta, N_{\mathrm{PV}}^{\mathrm{ref}}) \rangle, \tag{3}$$

where the brackets denote a statistical average over all events. In this case, the average is computed for events at each primary vertex multiplicity. At higher luminosities, or shorter τ_{bunch}, it may be necessary to use values $N_{\mathrm{PV}}^{\mathrm{ref}} > 1$ to account for a different calorimeter response.

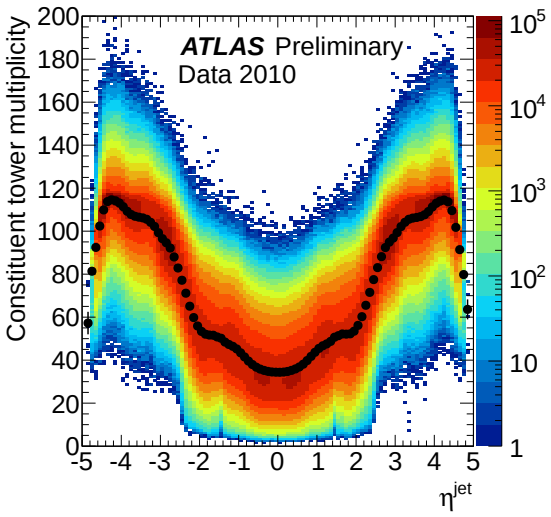

Figure 2: The number (various colours) and the average number (black circles) of noise-suppressed constituent calorimeter towers (constituent tower multiplicity) for anti-k_t jets with $R = 0.6$ and $p_T >$ 7 Gev as a function of η^{jet}.

The *tower-level* offset can be extrapolated to an EM scale *jet-level* offset by utilizing the average constituent tower multiplicity per jet given by Figure 2, yielding the jet-level offset for $R = 0.6$ shown in Figure 3(b). This jet-level offset is expressed as

$$\mathscr{O}_{\text{jet|tower}}(\eta, N_{\text{PV}}) = \mathscr{O}_{\text{tower-based}}(\eta, N_{\text{PV}}) \times \langle N^{\text{jet}}_{\text{towers}} \rangle, \tag{4}$$

where $\langle N^{\text{jet}}_{\text{towers}} \rangle$ is the mean constituent tower multiplicity obtained from Figure 2. The uncertainty associated with this extrapolation will be shown to be smaller than the impact of pile-up without the correction.

Additionally, the trigger selection itself results in a maximum fractional uncertainty on the tower-level offset shown in Figure 3(a) of approximately 16% (or a variation of 2.5 MeV per tower evaluated with respect to the median offset of 15 MeV per tower). This uncertainty was determined by comparing the measured energy distribution in calorimeter triggered events to events triggered via the minimum bias trigger scintillators. However, this variation in the analyzed data sample is constrained by the final closure tests shown in Section 6, and is taken into account in the systematic uncertainties via the overall variation in these tests.

5 Track-jet-based validation and offset correction

The track-jet approach utilizes jets constructed of charged particles, originating only from the selected pp collision of interest (see Section 3). Track-jets matched to the calorimeter jets provide a stable reference against which to compare calorimeter-jets by measuring the variation of the calorimeter $E^{\text{jet}}_{\text{T}}$ as a function of N_{PV}. It is therefore possible to both validate the tower-based offset correction (tower-level and jet-level) as well as to directly estimate the pile-up energy contribution to jets. As this method is only applicable to jets within the tracker acceptance, it serves primarily as a cross-check for the tower-based method discussed above. It can also be used, however, to derive a dedicated offset correction that can be applied to jets at energy scales other than the electromagnetic energy scale.

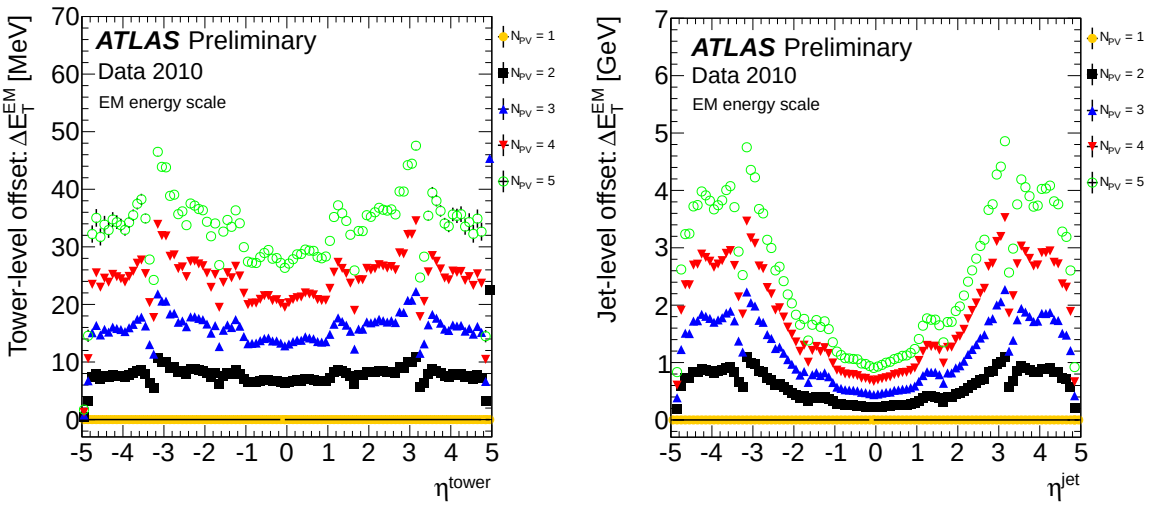

(a) (b)

Figure 3: (a) Tower-level offset at the electromagnetic (EM) scale and the (b) jet-level offset at the EM scale, each shown as a function of pseudorapidty and the number of reconstructed primary vertices.

5.1 Methodology

The technique consists of matching track-jets within a small $p_T^{\text{track-jet}}$ range with calorimeter jets and subsequently measuring the average calorimeter jet E_{T} versus N_{PV}. The matching criteria used for jets with $R = 0.6$ is

$$\Delta R(\text{jet}, \text{track-jet}) < 0.4, \tag{5}$$

where $\Delta R = \sqrt{\Delta\eta^2 + \Delta\phi^2}$. The offset is calculated in each of the 5 GeV bins in $p_T^{\text{track-jet}}$ as

$$\mathscr{O}_{\text{track-jet}} = \langle E_{\text{T}}^{\text{jet}}(N_{\text{PV}}|p_T^{\text{track-jet}})\rangle - \langle E_{\text{T}}^{\text{jet}}(N_{\text{PV}}^{\text{ref}}|p_T^{\text{track-jet}})\rangle. \tag{6}$$

For the purposes of the present study $N_{\text{PV}}^{\text{ref}} = 1$, but this may be extended to $N_{\text{PV}}^{\text{ref}} > 1$ for higher luminosity, short bunch-spacing operation in 2011-2012. Studying the variation of the offset as a function of the $p_T^{\text{track-jet}}$ range helps to establish the systematic uncertainty of the method. In addition, this approach has the advantage that it can be derived with the large di-jet sample available in the first data.

5.2 Track-jet based offset

Using the method described above, the transverse energy of the calorimeter jet is measured in six $p_T^{\text{track-jet}}$ ranges as a function of N_{PV}. Jets constructed from both noise-suppressed towers and topological clusters are used at both the EM and EM+JES energy scales.

Figure 4 displays the impact of pile-up on tower and topocluster jets at the EM scale, using the most probable value of a Landau convoluted with a Gaussian fit to the $E_{\text{T}}^{\text{jet}}$ distribution for each range of $p_T^{\text{track-jet}}$. In almost every case, a consistent offset of nearly $\mathscr{O} = 0.5$ GeV per vertex is found for $|\eta| < 1.9$, and no systematic trend of the offset as a function of $p_T^{\text{track-jet}}$ is observed, supporting the hypothesis that the offset correction is independent of $E_{\text{T}}^{\text{jet}}$. Typical errors for this differential offset are 20-50 MeV per

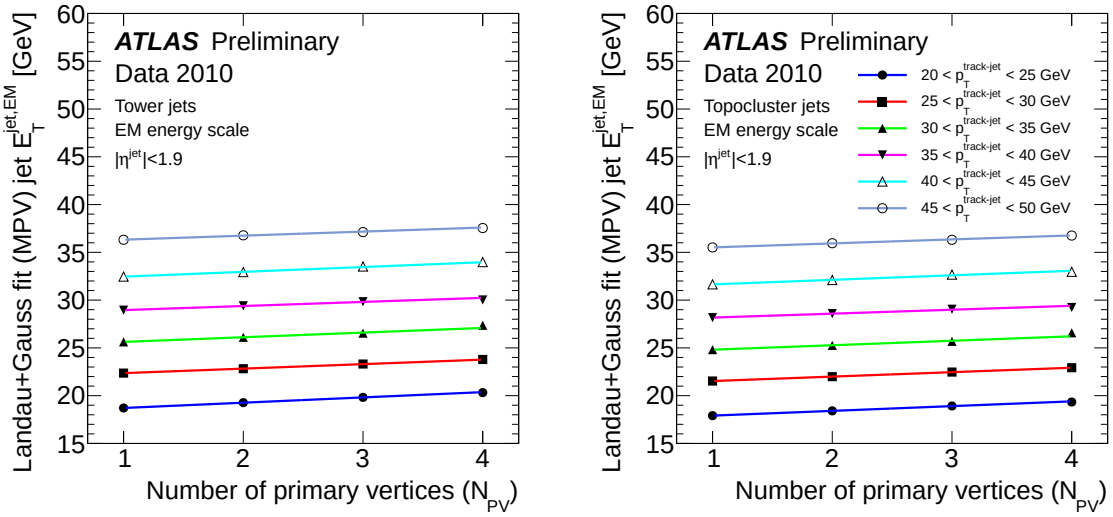

(a) Tower jets (EM scale, Landau+Gauss fit)

(b) Topocluster jets (EM scale, Landau+Gauss fit)

Figure 4: Jet $E_{\mathrm{T}}^{\mathrm{jet}}$ for calorimeter jets associated to track-jets as a function of $p_T^{\text{track-jet}}$ and the reconstructed vertex multiplicity, N_{PV}. Calorimeter jets are reconstructed at the EM scale with (a) noise-suppressed towers and (b) topological clusters. Both jet types exhibit a slope of approximately 0.5 GeV per vertex.

vertex, as shown in Table 1 in Section 6. A similar estimate of the jet-level offset using track-jets is performed at the EM+JES scale.

Figure 5 provides a summary of each of these results, presented in the form of the actual jet-level offset correction as a function of N_{PV} derived with respect to $N_{\mathrm{PV}}^{\mathrm{ref}} = 1$. The errors shown are statistical only. As expected, the magnitude of the offset is higher after calibration (Figures 5(c) and 5(d)), and the difference corresponds to the average jet energy scale correction received for jets with $p_T^{\mathrm{jet}} > 40$ GeV [12].

The track-jet approach offers the possibility to directly compute the offset correction, as shown in Figure 5. The variation of the offset among the various ranges of $p_T^{\text{track-jet}}$ indicates a systematic uncertainty on the correction of approximately $\delta(\mathscr{O}^{\mathrm{EM}}_{\mathrm{track-jet}}) < 100$ MeV per additional vertex at the EM scale and $\delta(\mathscr{O}^{\mathrm{EM+JES}}_{\mathrm{track-jet}}) < 200$ MeV per additional vertex at the EM+JES scale. Even when using this maximal EM scale systematic uncertainty, the application of the offset correction represents an improvement of a factor of five over the systematic bias associated with pile-up effects on the calorimeter jet transverse momentum.

6 Results

In this section, the results of closure tests of the tower-based offset correction, which apply the track-jet method to the corrected $E_{\mathrm{T}}^{\mathrm{jet}}$, are reported. In addition, the wide applicability of the tower-based offset correction is demonstrated by applying it to measurements of the differential jet shapes in events with two or three observed interactions.

6.1 Tower-based offset closure test using track-jets and discussion of uncertainties

The application of the offset correction shows reasonable closure at the tower-level and a slight under-correction at the jet-level, when evaluated using the most probable value of the corrected $E_{\mathrm{T}}^{\mathrm{jet}}$ distribution.

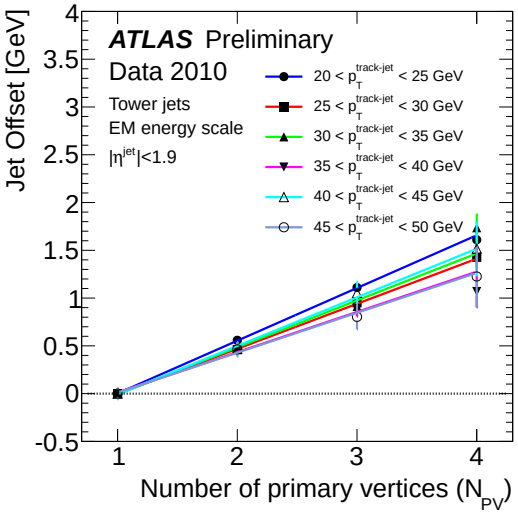

(a) Tower jet offset (EM scale)

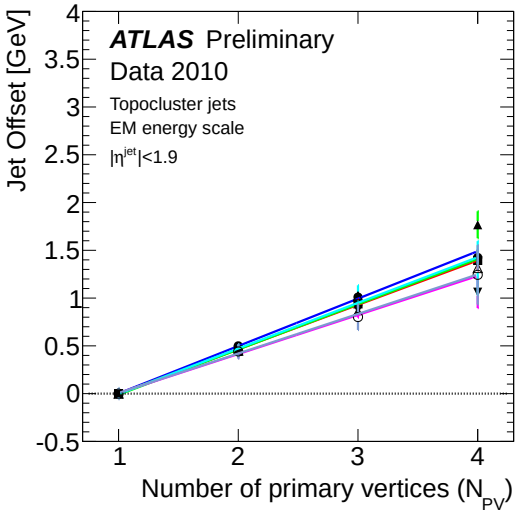

(b) Topocluster jet offset (EM scale)

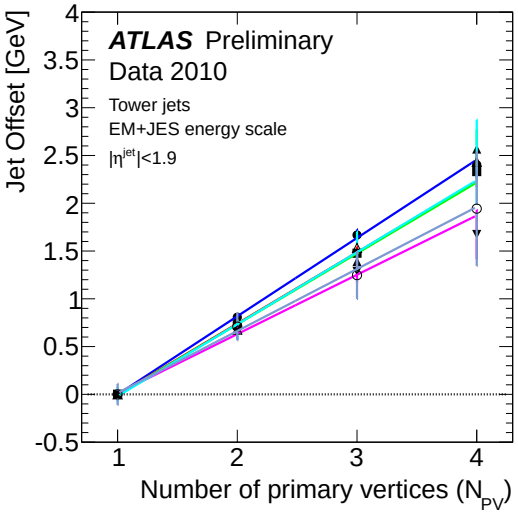

(c) Tower jet offset (EM+JES scale)

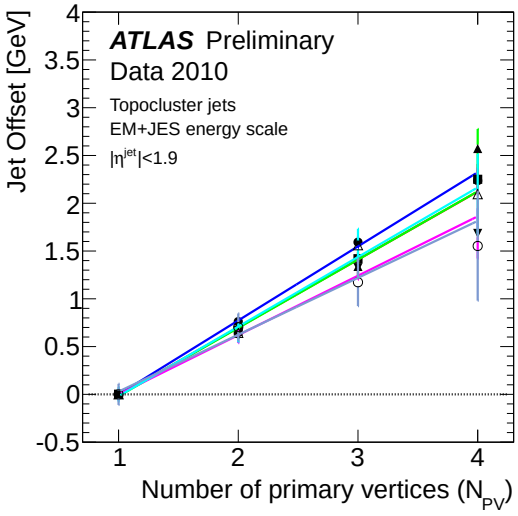

(d) Topocluster jet offset (EM+JES scale)

Figure 5: Direct measurements of the jet-level offset as a function of the number of interactions in the event for several ranges in $p_T^{\text{track-jet}}$. The track-jet offset is derived for (a) tower jets at the EM scale, (b) topocluster jets at the EM scale, (c) tower jets at the EM+JES scale, and (d) topocluster jets at the EM+JES scale. Errors shown are statistical only.

Figure 6(a) shows the tower-level correction applied to tower jets at the EM scale, as a function of the reconstructed vertex multiplicity. At this level, the correction makes use of the actual constituent tower multiplicity in each jet. Figure 6(b) and Figure 6(c) show the jet-level correction applied to both tower jets and topocluster jets, respectively. In the case of the jet-level correction, the average constituent tower multiplicity mode presented in Section 4 is used. The tower-level correction exhibits a closure consistent with zero slope in $E_{\mathrm{T}}^{\mathrm{jet}}$ as a function of N_{PV}. However, the use of the jet-level offset correction slightly under-corrects for the effect of pile-up for jets constructed from *both* towers and topoclusters.

The implication of this observation is two-fold:

- There is no significant difference in the susceptibly of topological cluster jets to pile-up as compared to tower jets.
- There is a systematic underestimation of the tower multiplicity in jets due to both the assumed $E_{\mathrm{T}}^{\mathrm{jet}}$ spectrum and the effect of pile-up.

Track-jet p_T ($p_T^{\text{track-jet}}$)	Tower jets [GeV/vertex]		Topocluster jets [GeV/vertex]	
	Before	After	Before	After
20 - 25 GeV	0.55 ± 0.02	0.06 ± 0.02	0.50 ± 0.02	0.19 ± 0.02
25 - 30 GeV	0.47 ± 0.02	0.00 ± 0.02	0.47 ± 0.02	0.16 ± 0.02
30 - 35 GeV	0.49 ± 0.03	0.01 ± 0.03	0.47 ± 0.03	0.17 ± 0.03
35 - 40 GeV	0.42 ± 0.03	-0.08 ± 0.03	0.41 ± 0.03	0.12 ± 0.03
40 - 45 GeV	0.51 ± 0.05	0.01 ± 0.05	0.48 ± 0.05	0.18 ± 0.05
45 - 50 GeV	0.42 ± 0.06	-0.07 ± 0.06	0.41 ± 0.06	0.12 ± 0.06
Average	0.48 ± 0.02	-0.01 ± 0.02	0.46 ± 0.02	0.16 ± 0.02

Table 1: Variation of the calorimeter $E_{\mathrm{T}}^{\mathrm{jet}}$ with pile-up. Slopes are given in GeV/vertex at the EM scale for each pile-up vertex in the event, and represent the slope of the jet offset before and after the tower-based offset correction. Both tower-level and jet-level corrections are shown, applied to tower jets and topocluster jets, respectively. The reported errors are purely statistical.

The systematic uncertainties on the offset correction are estimated from the variation of the tower-multiplicity, trigger selection, the variation of the offset derived from the track-jet method (Section 5), and finally from the result of the closure test. Each systematic uncertainty is summarized in Table 2 and expressed as a percentage of the average offset correction, shown in Table 1.

For the tower-level offset correction, in which the constituent towers themselves are used, the quadrature sum of each systematic uncertainty is significantly larger than the closure test indicates. The larger of the two individual uncertainties is therefore adopted, or $\delta(\mathscr{O}^{\text{tower-level}}) = 100$ MeV per vertex for the tower-level correction[4]. The resulting total uncertainty is a factor of five smaller than the bias attributable to pile-up ($\mathscr{O} \approx 500$ MeV per vertex) even while using a very conservative systematic uncertainty.

It is important to note that the jet-level offset correction receives an additional uncertainty due to the average tower multiplicity approximation. This contribution is estimated to introduce a 20% variation in the constituent tower multiplicity by comparing jets in events with $N_{\mathrm{PV}} = 1-3$ and for the five highest $p_T^{\text{track-jet}}$ bins, which translates directly into a 20% uncertainty on the jet-level offset. The resulting systematic uncertainty on jets corrected by the jet-level offset correction (topological cluster jets) is estimated to be $\delta(\mathscr{O}^{\text{jet-level}}) \approx 160$ MeV per vertex, a factor of three smaller than the bias due to pile-up.

[4]Using twice the RMS of the variation in the closure test yields the same value.

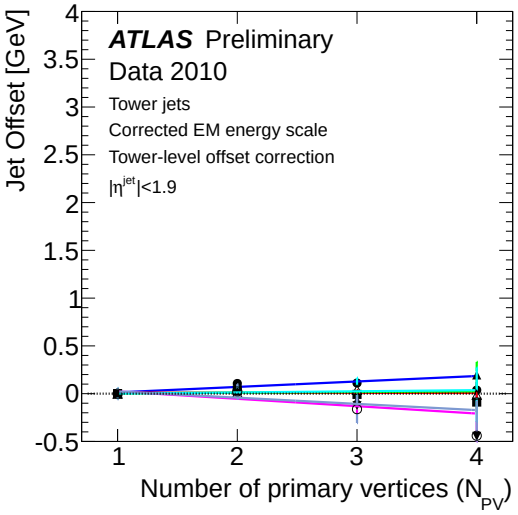

(a) Tower jets with EM scale tower-level correction

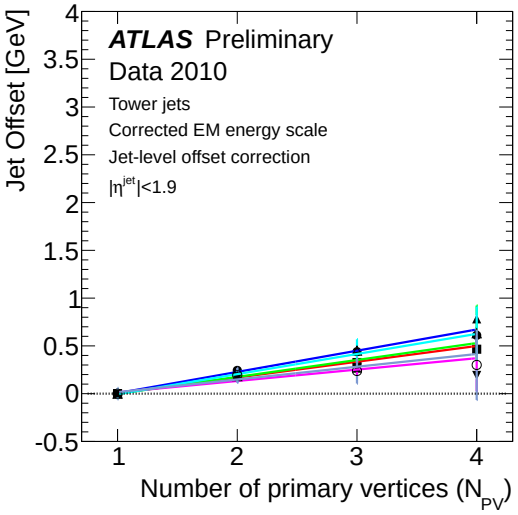

(b) Tower jets with EM scale jet-level correction

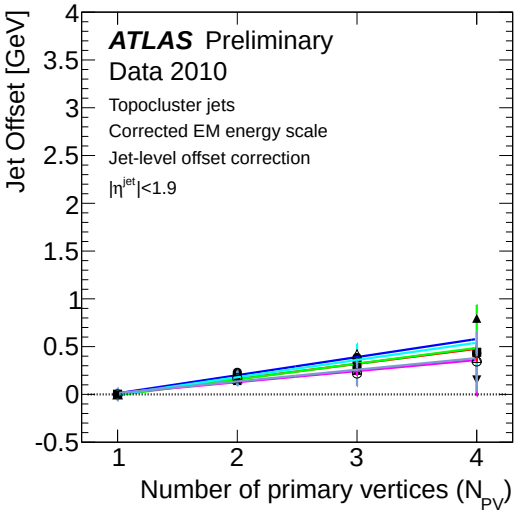

(c) Topocluster jets with EM scale jet-level correction

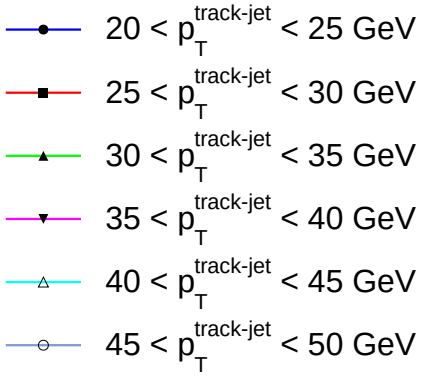

(d)

Figure 6: Closure tests of the offset correction at the EM scale using the fitted (Landau+Gauss fits) $E_{\mathrm{T}}^{\mathrm{jet}}$ most probable value (MPV) for various track-jet $p_T^{\text{track-jet}}$ bins for (a) tower jets corrected with tower-based offset correction, (b) tower jets corrected with the jet-level offset correction and (c) topocluster jets corrected with the jet-level offset correction. The axis ranges are identical to Figure 5 for ease of comparison.

Systematic	Tower-level offset	Jet-level offset	Comments
Tower multiplicity variation	–	20%	$\langle N_{\text{towers}}^{\text{jet}} \rangle$ vs. $p_T^{\text{track-jet}}$ and N_{PV}
Trigger selection	16%	16%	MinBias vs. Calo triggers
$p_T^{\text{track-jet}}$ variation	21%	22%	Variation of 100 MeV/vertex
Total (quadrature sum)	26%	34%	Assumes uncorrelated errors
Result from closure test	2%	35%	Determined from average

Table 2: Summary of systematics associated with the offset correction for both the tower-level offset and the jet-level offset correction variants. The uncertainty is expressed as a percentage of the average offset correction, shown in Table 1.

6.2 Tower-based offset correction applied to jet shapes measurements

Finally, in order to assess the applicability of the tower-based offset outside of the narrow context of jet response, the correction is applied to the measurement of the differential jet shape for $R = 0.6$ tower jets, as described in [17, 18].

The jet shape variable used, $\rho^a(r)$, is defined as:

$$\rho^a(r) = \frac{1}{\pi\left[(r+\delta r/2)^2 - (r-\delta r/2)^2\right]} \times \left\langle \frac{p_T\left(r-\frac{\delta r}{2}, r+\frac{\delta r}{2}\right)}{p_T(0,0.7)} \right\rangle \tag{7}$$

where the angled brackets denote an average over all jets, $p_T(b,c)$ is the sum of the p_T of all noise-suppressed towers with an opening angle $b < \Delta R < c$ with respect to the jet axis, and $\delta r = 0.1$. This definition differs from the canonical jet shape variable $\rho(r)$ in two important ways. First, by normalizing to area, the variable measures an energy density. Therefore, $\rho^a(r)$ will approach an asymptotic value far from the jet axis. The level of the asymptote is related to the energy density in the calorimeter and is measurably higher in events with pile-up. Second, all noise-suppressed towers (not just the constituents of the jet) are included in the definition. This allows an examination of energy outside of the jet cone, in some sense measuring "energy flow" around the jet axis.

Figure 7 depicts $\rho^a(r)$ at detector level with and without the offset correction, and for events with more than one reconstructed vertex. In events with 2 (3) reconstructed vertices, differences in this particular jet shape variable of up to 35% (70%) just outside the jet ($r > 0.6$) and 20% (40%) near the nominal jet radius ($r = 0.6$) are observed. The bulk of the shape ($0.1 < r < 0.6$) is restored to that observed in events with only a single interaction, as well as both the core ($r < 0.1$) and the periphery ($r > 0.6$) of the jet.

The results demonstrate that the tower-based offset correction can be applied on a fine scale granularity and is applicable both inside and *near* jets. The possibilities for correcting the jet shape in both direct QCD physics measurements and for searches for beyond the Standard Model physics using jet substructure are very promising.

7 Conclusions

A multi-faceted *in-situ* approach is presented for correcting the jet energy scale for the presence of multiple proton-proton interactions in the same event. The uncorrelated energy contributed to a jet in such events can be reliably estimated, *on average*, via both tower-based and track-jet methods using the measured number of primary vertices. Using the track-jet method as a validation tool for the tower-based offset correction, the impact on the jet energy scale is reduced by a factor of five over the measured

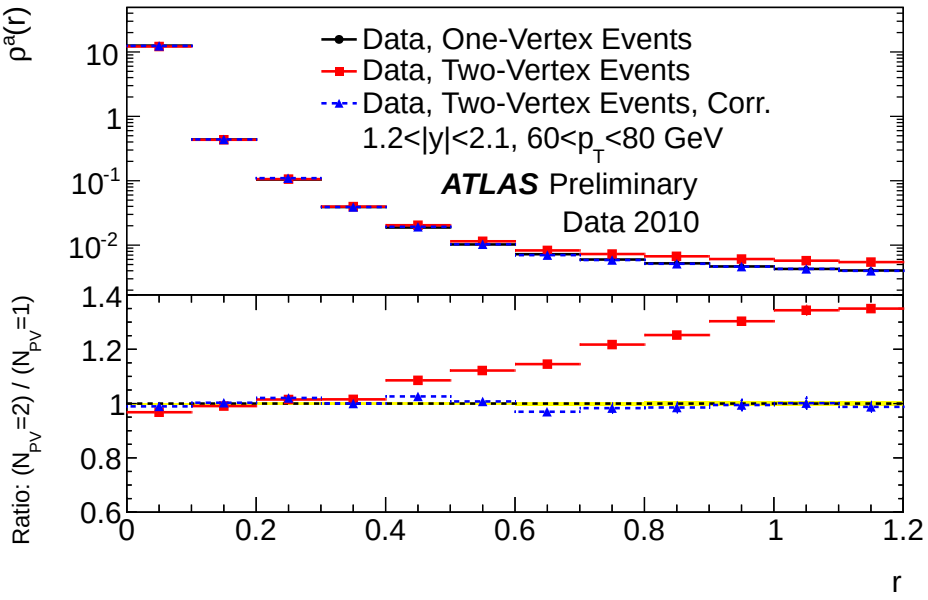

(a) Comparison of $N_{\mathrm{PV}} = 1$ and 2 ($1.2 < |y^{\mathrm{jet}}| < 2.1$)

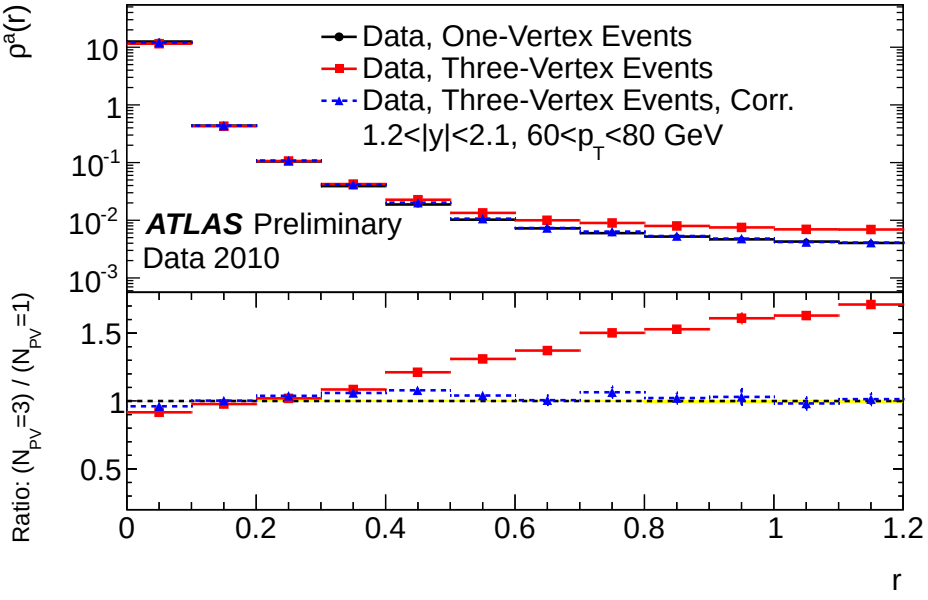

(b) Comparison of $N_{\mathrm{PV}} = 1$ and 3 ($1.2 < |y^{\mathrm{jet}}| < 2.1$)

Figure 7: Measured sum p_T in annuli around the jet axis, divided by the total p_T around the jet, and normalized by the area of each annulus. Events are selected with more than one reconstructed vertex. The shapes of jets in the rapidity range $1.2 < |y^{\mathrm{jet}}| < 2.1$ are compared, before and after the offset corrections, in events with (a) one and two vertices, and (b) one and three vertices. The corrected distribution is also shown (blue triangles). Note that the single vertex data (black circles) are partially hidden behind the corrected multi-vertex data.

bias due to multiple collisions for jets built from noise-suppressed towers and by a factor of three for topological cluster jets. The resulting systematic uncertainty is approximately 100 MeV (160 MeV) per vertex for anti-k_t $R = 0.6$ tower (topological cluster) jets in the central region up to $|\eta| < 1.9$. The average jet-level EM scale offset correction shows very good performance but could benefit from improvements in the method of extrapolation from the tower to the jet-level.

Furthermore, the track-jet method provides the ability to derive an offset correction for jets at any energy scale and for any input constituent type. The determination of systematic uncertainties becomes slightly more difficult, in this case, due to the lack of an independent validation tool, but work is underway to develop this approach as fully as the tower-based correction has been.

Finally, the application of the offset correction in the context of jet shapes is studied. By applying the tower-level correction to the energy in annuli around the jet axis in events with more than one interaction, effects of up to 40% near the jet periphery are completely removed as compared to events with only a single observed collision. This result presents the very real prospect of using the tower-based offset correction not only to improve the jet energy measurements, but also to directly enhance physics measurements involving the jet shape and jet substructure.

References

[1] O. Bruning, *LHC challenges and upgrade options*, J. Phys.: Conf. Ser. **110 112002** (2010) .

[2] M. Lamont, *LHC status and plans*, in proceedings of the XVIII International Workshop on Deep-Inelastic Scattering and Related Subjects **PoS(DIS 2010)012** (2010) .

[3] ATLAS Collaboration, G. Aad et al., *The ATLAS Experiment at the CERN Large Hadron Collider*, JINST **3** (2008) S08003.

[4] M. Cacciari and G. P. Salam, *Pileup subtraction using jet areas*, Physics Letters B **659** (2008) no. 1-2, 119 – 126.

[5] R. Alon, E. Duchovni, G. Perez, A. P. Pranko, and P. K. Sinervo, *A data-driven method of pile-up correction for the substructure of massive jets*, hep-ph/1101.3002 (2011) , arXiv:1101.3002 [hep-ph].

[6] ATLAS Collaboration, G. Aad et al., *Luminosity Determination in pp Collisions at* $\sqrt{s} = 7$ *TeV Using the ATLAS Detector at the LHC*, hep-ex/1101.2185, submitted to EPJC (2011) , arXiv:1101.2185 [hep-ex].

[7] M. Ferro-Luzzi, *2010 Experiences and Expectations for 2011*, The LHC Beam Operation workshop **Workshop proceedings** (Dec, 2010) .

[8] ATLAS Collaboration, *Performance of the ATLAS Jet Trigger in the Early* $\sqrt{s} = 7$ *TeV Data*, ATLAS Note **ATLAS-CONF-2010-094** (Oct, 2010) .

[9] M. Cacciari, G. P. Salam, and G. Soyez, *The anti-k_t jet clustering algorithm*, JHEP **04** (2008) 063, arXiv:0802.1189 [hep-ph].

[10] M. Cacciari and G. P. Salam, *Dispelling the N^3 myth for the k_t jet-finder*, Phys. Lett. **B659** (2008) 119–126, arXiv:0707.1378 [hep-ph].

[11] W. Lampl et al., *Calorimeter clustering algorithms: description and performance*, ATLAS Note **ATL-LARG-PUB-2008-002** (Apr, 2008) .

[12] ATLAS Collaboration, *Jet energy scale and its systematic uncertainty in ATLAS for jets produced in proton-proton collisions at* $\sqrt{s} = 7$ *TeV*, ATLAS Note **ATLAS-CONF-2010-056** (Jul, 2010) .

[13] ATLAS Collaboration, G. Aad et al., *Charged-particle multiplicities in pp interactions measured with the ATLAS detector at the LHC*, hep-ex/1012.5104, accepted by NJP (2011) , arXiv:1012.5104 [hep-ex].

[14] ATLAS Collaboration, *Characterization of Interaction-Point Beam Parameters Using the pp Event-Vertex Distribution Reconstructed in the ATLAS Detector at the LHC*, ATLAS Note **ATLAS-CONF-2010-027** (Jul, 2010) .

[15] ATLAS Collaboration, *Performance of primary vertex reconstruction in proton-proton collisions at* $\sqrt{s} = 7$ *TeV in the ATLAS experiment*, ATLAS Note **ATLAS-CONF-2010-069** (Jul, 2010) .

[16] ATLAS Collaboration, *Properties of Jets and Inputs to Jet Reconstruction and Calibration with the ATLAS Detector Using Proton-Proton Collisions at* $\sqrt{s} = 7$ *TeV*, ATLAS Note **ATLAS-CONF-2010-053** (Jul, 2010) .

[17] Z. L. Marshall, *A Measurement of Jet Shapes in Proton-Proton Collisions at 7.0 TeV Center-of-Mass Energy with the ATLAS Detector at the Large Hadron Collider*. *CERN-THESIS-2010-142*. PhD thesis, Pasadena, CA, USA, California Institute of Technology, 2010. Presented on 09 Nov 2010.

[18] ATLAS Collaboration, G. Aad et al., *Study of Jet Shapes in Inclusive Jet Production in pp Collisions at* $\sqrt{s} = 7$ *TeV using the ATLAS Detector*, hep-ex/1101.0070, Accepted by Phys Rev. D (2011) , arXiv:1101.0070 [hep-ex].